Carbohydrate Polymers 101 (2014) 272–280

Contents lists available at ScienceDirect

Carbohydrate Polymers

journal homepage: www.elsevier.com/locate/carbpol

High strength of hemicelluloses based hydrogels by freeze/thaw technique

Ying Guan [a], Jing Bian [a], Feng Peng [a,*], Xue-Ming Zhang [a], Run-Cang Sun [a,b,**]

[a] Beijing Key Laboratory of Lignocellulosic Chemistry, College of Materials Science and Technology, Beijing Forestry University, Beijing 100083, China
[b] State Key Laboratory of Pulp and Paper Engineering, South China University of Technology, Guangzhou 510640, China

ARTICLE INFO

Article history:
Received 16 July 2013
Received in revised form 23 August 2013
Accepted 25 August 2013
Available online 12 September 2013

Keywords:
Hemicelluloses
Polyvinyl alcohol
Chitin nanowhiskers
Hydrogel
Freeze/thaw cycle

ABSTRACT

Novel hydrogels were prepared from hemicelluloses, polyvinyl alcohol (PVA), and chitin nanowhiskers through 0, 1, 3, 5, 7, and 9 times of freeze/thaw cycle. These hydrogels were characterized by Fourier transform infrared spectroscopy (FT-IR), scanning electron microscopy (SEM), X-ray diffraction (XRD), thermo-gravimetric analysis (TGA), swelling property, and compressive strength. The repeated freeze/thaw cycles induced physically crosslinked chains packing among these polymers, and a phase separation caused by the hydrogen bonds. Larger pores led to a high swelling degree, whereas the formation of compact structure after multiple freeze/thaw cycles resulted in high mechanical strength and thermal stability. The highest compressive strength of these hydrogels was achieved by the 9 times of freeze/thaw cycles with compressive stress of 10.5 MPa. This work provides a remarkable way for the preparation of hydrogels with good mechanical properties by physical method.

1. Introduction

Polymers from renewable resources are receiving increased attention in the scientific community because of projected shortage of petroleum-based raw materials in the near future (Muzaffer, Mandla, Daniel, & Gisela, 2011). Hemicelluloses, comprising the non-cellulose cell-wall polysaccharides of plants, are the second most abundant polysaccharides in biomass. Since hydrogels have inherent hydrophilicity, low toxicity or non-toxicity, biodegradability, and biocompatibility, the formation has been a potential area of application for hemicelluloses and their derivatives (Galeska et al., 2005; Liu, Lin, Li, & Liu, 2005; Nishi & Jayakrishnan, 2007). Hemicelluloses are suitable for different applications in tissue engineering and drug delivery systems because of their peculiar physicochemical properties, such as biocompatibility (Coviello, Matricardi, Marianecci, & Alhaique, 2007; Lindblad, Sjoberg, Albertsson, & Hartman, 2007). Polyvinyl alcohol (PVA) has several good properties including non-toxicity, biocompatibility, high hydrophilicity, fiber/film forming ability, and chemical and mechanical resistance. It has been widely commercialized in the chemical and medical industry for the production of fiber, film, coating, cosmetic, pharmaceutical, and so on (Yeo et al., 2000). As renewable and biodegradable nanoparticles, chitin whiskers are attracting attention from both academic and industrial fields. Within or without modification, they had found extensive applications in many areas including reinforcing nanocomposites, cosmetic, food industry, drug delivery, tissue engineering (Tamuraa, Furuikea, Nairb, & Jayakumar, 2011; Zeng, He, Li, & Wang, 2012), and were reported to reinforce polymer nanocomposites nanofibers (Junkasem, Rujiravanit, Grady, & Supaphol, 2010; Junkasem, Rujiravanit, & Supaphol, 2006).

Every year, millions of people suffer from loss of life or other health-related tissues associated with organ failure (Slaughter, Khurshid, Fisher, Khademhosseini, & Peppas, 2009). Due to limitations with the number of available organ donors, there is an increasing demand for artificial tissue replacements (Camci-Unal, Alemdar, Annabi, & Khademhosseini, 2013). As early as 1975, Peppas et al. had succeeded in producing strong PVA hydrogel by the freeze/thaw method and using it as an artificial cartilage (Peppas, 1975, 1979). However, the mechanical strength of this PVA hydrogel was thought to be too weak to use as a joint material by Ushio et al. (2004).

Hydrogels are water-swollen polymeric materials that maintain a distinct three-dimensional structure (Wichterle & Lím, 1960), while absorbing a large amount of water, thus they have been widely investigated for facilitating the controlled release of a variety of clinically-relevant drugs (Andrade-Vivero, Fernandez-Gabriel, Alvarez-Lorenzo, & Concheiro, 2007; Bos et al., 2004; Bouhadir, Kruger, Lee, & Mooney, 2000; Hoare & Kohane, 2008).

* Corresponding author. Tel.: +86 1062336903 00; fax: +86 1062336903 00.
** Corresponding author at: Beijing Key Laboratory of Lignocellulosic Chemistry, Beijing Forestry University, Beijing 100083, China. Tel.: +86 1062336903 00; fax: +86 1062336903 00.
E-mail addresses: fengpeng@bjfu.edu.cn (F. Peng), rcsun3@bjfu.edu.cn (R.-C. Sun).

0144-8617/$ – see front matter © 2013 Elsevier Ltd. All rights reserved.
http://dx.doi.org/10.1016/j.carbpol.2013.08.085

Hydrogels have found particular utility in the area of controlled release since they can be loaded with high fractions of drugs due to their high internal free volume and can be fabricated to have similar physical, mechanical, and chemical properties to native extracellular matrix, which generally results in high biocompatibility in a variety of biological environments (Cai, Liu, Zheng, & Prestwich, 2005).

Hydrogels can be either physically or chemically cross-linked and are rendered insoluble due to the presence of these chemical, covalent, ionic or physical cross-links (Michael, Clement, Luke, & Michael, 2009). The freeze/thaw technique, as the physical method, has a remarkable advantage of being able to crosslink the polymer solutions without leaving in the gel matrix any crosslink remnant which could leak out and evoke serious inflammatory response after implantation into the human body (Liu, Vrana, Cahill, & McGuinness, 2009). The quenching at low temperature, during the freezing step, induces a liquid–liquid phase separation and the formation of ice crystals in polymer-poor phase. The ice crystals, in turn, expel amorphous polymer segments, increasing the polymer concentration in the surrounding environment. The size of ice crystals formed in the polymer-depleted pockets increases by the repeated freeze/thaw cycles. The size of phase-separated domains is of the order of microns, thus accounting for the opaque aspects of the hydrogels. Upon thawing, the ice crystals melt, leaving the porous structure of the hydrogel unaltered. Practically, water works as a porogen in the solution of polymers, whereas the polymer network increases its stability during the freezing step (Chen, Park, & Park, 1999; Hassan & Peppas, 2000; Lozinsky, 1998; Oxley, Corkhill, Fitton, & Tighe, 1993).

The hydrogels were formed with hemicelluloses, PVA, and chitin nanowhiskers by freeze/thaw cycle have not been reported yet. Chitin whiskers in the hemicelluloses/PVA matrix enhance the mechanical strength due to the formation of hydrogen bonds among the three polymers. For freeze/thaw method, several parameters affect the final properties of hydrogels, such as repeated cycles, polymer concentration, and reaction time. In this paper, we present a new strategy for blending of hemicelluloses, PVA, and chitin nanowhiskers by physical crosslinking of freeze/thaw method with different repeated times. The structure and morphology of the hydrogels were characterized by SEM, XRD, TGA, FT-IR, swelling property, and compression strength.

2. Experimental

2.1. Materials

PVA (degree of polymerization was 1750 ± 50) were purchased from Beijing Yili Fine Chemicals Co., Ltd. China. α-Chitin was supplied by Zhejiang Golden-Shell Biochemical Co., Ltd., China. The weight-average molecular weight (Mw) was 5.0×10^5. Its degree of acetylation (DA) was calculated to be 73% from the nitrogen content in terms of DA (%) = $1 - [(W_C/W_N - 5.14)/1.72] \times 100$ (Tang, Zhou, & Zhang, 2012). All the reagents used were of analytical grade.

2.2. Preparation of hemicelluloses

Hemicelluloses were extracted from bamboo (*Phyllostachys pubescens*) holocellulose with 5 w/v% NaOH at 60 °C for 4 h with a solid to liquid ratio of 1:25 (g mL^{-1}). The holocellulose was obtained by delignification of the extractive-free bamboo (40–60 mesh) with 6% sodium chlorite in acidic solution (pH 3.6–3.8, adjusted by 10% acetic acid) at 75 °C for 2 h. The holocellulose was subsequently extracted with 5% NaOH at 50 °C for 8 h. The filtrate was neutralized with 6.0 M HCl to pH 5.5, dialyzed (7.0 kDa cutoff) until free of NaCl, concentrated, and precipitated with three volumes of ethanol. The precipitated hemicellulose were obtained by centrifugation (4000 rpm, 15 min), re-dissolved in distilled H_2O, and then freeze-dried. The sugar composition of the hemicelluloses was: 83.6% xylose, 5.1% arabinose, 4.2% glucose, 0.4% galactose, and 6.8% glucuronic acid (relatively molar percent). The molecular weight obtained by gel permeation chromatography (GPC) (Peng et al., 2009) showed that the native hemicelluloses had a weight average molecular weight (Mw) of 13 420 g mol^{-1} with a polydispersity of 4.1, corresponding to a degree of polymerization of 88.

2.3. Preparation of chitin nanowhiskers

The raw chitin powder was treated with 1 mol L^{-1} NaOH (room temperature, overnight), then 0.3 w/v% $NaClO_2$ (buffered to pH 4.0, 80 °C, 3 h), and washed with water after each step. These treatments were repeated twice. Purified chitin powder was freeze-dried and kept in a desiccator. The purified chitin was hydrolyzed in 3 mol L^{-1} HCl at 90 °C for 1.5 h to digest the disordered regions and decrease particle size. After acid hydrolysis, the suspensions were diluted with deionized water, followed by centrifugation and decanting the supernatant. This process was repeated three times. After that, the chitin was recovered by centrifugation and resuspended in distilled water to reduce the acid concentration. The obtained chitin suspension was dialyzed against flowing tap water for 2 h and then dialyzed against distilled water for 12 h. Dialysis was performed with dialysis membrane (8–14 KDa cutoff). At last, the chitin suspension was freeze-dried.

2.4. Preparation of hydrogels

1.5 g PVA was dissolved in 40 mL distilled water at 90 °C with vigorous stirring for 30 min. Then, 1.5 g hemicelluloses and 1.5 g chitin nanowhiskers were suspended in 80 mL distilled water. The 10 mL mixed solution (3.75 w/w%) with the proportion of 1:1:1 was stirred vigorously at room temperature and heated slowly up to 80 °C for 1 h. After cooling to room temperature, the mixtures were poured into a Teflon mold, frozen at −20 °C for 10 h, and subsequently thawed for 1 h at room temperature. The hydrogels were obtained after the freeze/thaw cycle repeated for 0, 1, 3, 5, 7, and 9 times, and coded as Gel-0, Gel-1, Gel-3, Gel-5, Gel-7, and Gel-9, respectively.

2.5. Characterization

The freeze-dried sample was diluted 10,000 times by distilled water. The surface of chitin nanowhiskers was studied by AFM (Nanoscope III, Veeco). In the AFM scanning, two to four interest locations on each sample were tested. Small pieces of samples were glued onto metal disks and attached to a magnetic sample holder located on the top of the scanner tube. Topographic (height) and phase images were recorded under ambient air conditions. All images were recorded in tapping mode in air using silicon cantilevers with a resonance frequency between 250 and 300 kHz, and a scan angle of 0°.

SEM of the hydrogel samples were carried out with a Hitachi S-3400N II (Hitachi, Japan) instrument at 15 kV. Prior to taking pictures, the samples were sputter-coated with a thin layer of gold. Images were obtained at magnifications ranging from 200× to 5000× which was dependent on the feature to be traced.

The crystallinities of the PVA, chitin nanowhiskers, and hydrogels were measured using an XRD-6000 instrument (Shimadzu, Japan) with a Cu Kα radiation source ($\lambda = 0.154$ nm) at 40 kV and 30 mA. Samples were scanned from 5° to 40° (2θ) at a speed of 2° min^{-1}.

FT-IR spectra of the hydrogels were recorded using a Thermo Scientific Nicolet iN 10 FT-IR Microscope (Thermo Nicolet Corporation, Madison, WI) equipped with a liquid nitrogen cooled MCT detector. Dried samples were ground and palletized using BaF_2 and their spectra were recorded from 4000 to 650 cm^{-1} at a resolution of 4 cm^{-1} and 128 scans per sample.

Thermal analysis was performed by using TGA and on a simultaneous thermal analyzer (PyrisDiamond TG/DTA, PE Instrument). The apparatus was continually flushed with nitrogen. The sample weighed between 9 and 11 mg was heated from room temperature to 700 °C at a heating rate of 10 °C min^{-1}.

The undried hydrogel samples were 5 mm × 10 mm (diameter × height) in dimension and incubated in distilled water for 24 h at 25 °C before the test. Compression test of hydrogels was performed on a CMT6503 Test Machine (ShenZhen SANS, China), with a speed of 5 mm min^{-1} according to ISO527-1995(E).

The weighted freeze-dried hydrogels were immersed into excessive distilled water to reach a state of equilibrium swelling. The swollen superabsorbent was filtered using 100-mesh sieve and drained for 20 min until no free water remained. After weighing the swollen hydrogels, the equilibrium water absorption was calculated by using the following equation:

$$Q_{eq} = \frac{W_2 - W_1}{W_1}$$

where Q_{eq} is the equilibrium water absorption defined as grams of water per gram of sample; W_1 and W_2 are the mass of sample before and after swelling, respectively.

3. Results and discussion

3.1. Morphological analysis

AFM technique was used to observe the external surface of α-chitin. The images of the α-chitin after acid hydrolysis are shown in Fig. 1. As it can be seen, the α-chitin displayed slender rods with the length of 200 ± 10 nm and width of 40 ± 10 nm, respectively. Rod-like chitin nanowhiskers was produced. Because of the colloidal behavior of the nanowhiskers and no observation of a precipitation after mixing chitin nanowhiskers with hemicelluloses/PVA aqueous solution, the nanowhiskers dispersed uniformly in the matrix and a freeze/thaw technique could be used for fabricating the hydrogels.

The preparation principle of chitin nanowhiskers is on the basis of the different hydrolytic kinetics between amorphous and crystalline domains (Habibi, Lucia, & Rojas, 2010). That is to say, both the amorphous and crystalline phases of chitin can be hydrolyzed during the treatment with acid aqueous solutions. The swelling and hydrolysis of amorphous phases occurred much faster than those of crystalline phases due to the periodic tight arrangement of molecular chains in the crystalline domains. It is known that the treatment of chitin in heating HCl can dissolve the amorphous domains of chitin; however, it can also break the ether and amide linkages of chitin (Clark & Smith, 1936; Saito, Putaux, Okano, Gaill, & Chanzy, 1997). Therefore, after removal of the amorphous domains, the surface of crystallites will be attacked by the excess acid and thus undergo further hydrolysis. Thus, controlling the hydrolytic extent of chitin is very important for the preparation of chitin nanowhiskers with desired size and good yield. When 3 mol L^{-1} HCl was applied, the chitin of nanometer level was obtained, whereas the structure of α-chitin was not destroyed significantly.

As seen in Fig. 2(a–f), SEM images of hydrogels with porous network structures which formed by hemicelluloses/PVA/chitin nanowhiskers by freeze/thaw cycles for 0, 1, 3, 5, 7, and 9 times are presented. A spider-web pattern (Fig. 2b) was presented in the cross-section of the hydrogel only after one freeze/thaw cycle, which decreased with the increment of the freeze/thaw cycles, and finally disappeared in hydrogels obtained by 5 cycles as shown in Fig. 2d. It was found that the hydrogen-bonded

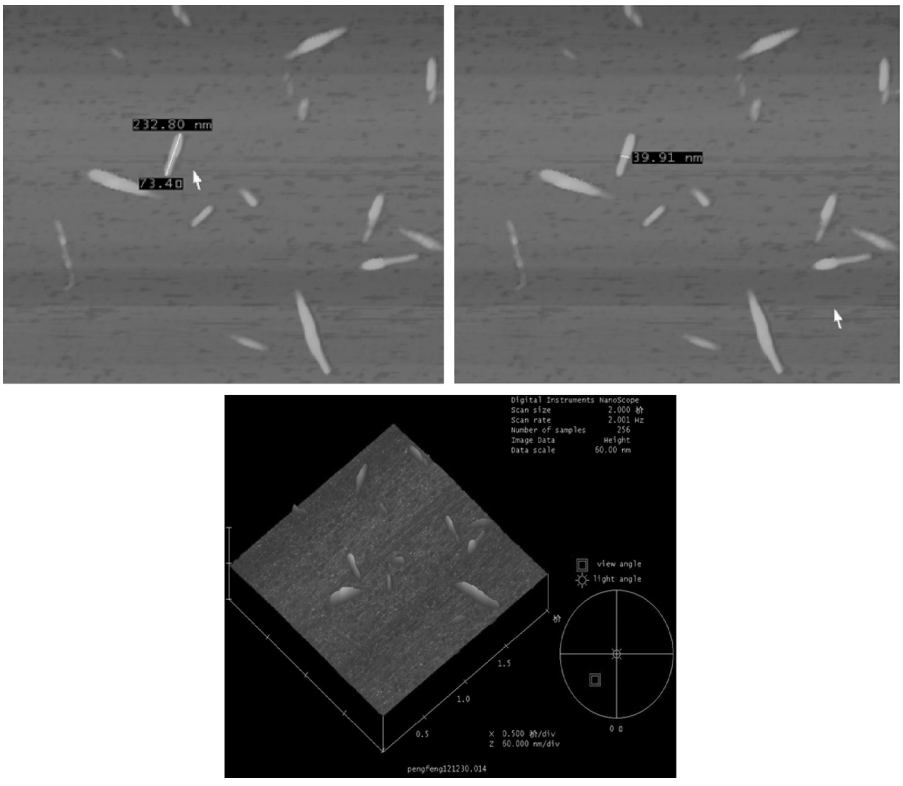

Fig. 1. AFM images of α-chitin nanowhiskers after acid hydrolysis.

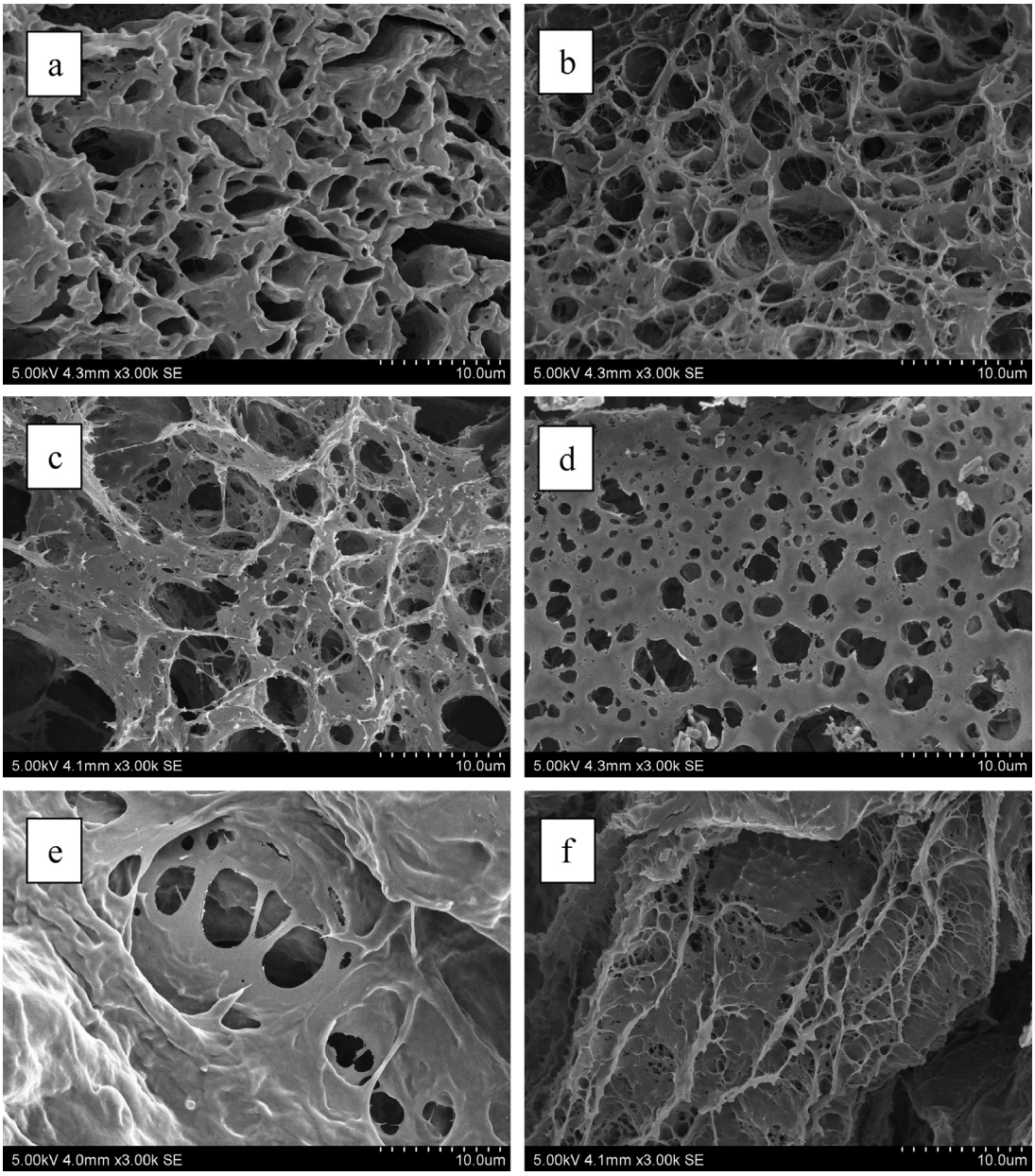

Fig. 2. SEM images of Gel-0, Gel-1, Gel-3, Gel-5, Gel-7, and Gel-9 (a–f).

networks among hemicelluloses, PVA, and chitin nanowhiskers were easy to form, because these polymers had abundant hydroxyl bonds and the hydrogen-bonded network structures were at a highly stable state under low temperature. However, an interesting pattern, resembling a lamellar structure with honeycomb-like pore, was found in Gel-5. The linking bridges among lamellar structures appeared ruptured and irregular, which might be produced by the intrinsic pressure of ice crystal after freezing.

The hemicelluloses, PVA, and chitin nanowhiskers were promoted to combine into the chains packing during the freezing process. Their molecular chains could associate more compactly to form the physically crosslinked chains packing with the increase of the freeze/thaw cycles, which led to the tough pore wall in the hydrogel structure. Upon thawing, a phenomenon known as syneresis occurs because the water can be easily expressed from the dense networks.

3.2. Structure analysis

X-ray diffraction patterns of the hydrogels formed by PVA/hemicelluloses/chitin nanowhiskers with 0, 3, 7, and 9 times of freeze/thaw cycle are depicted in Fig. 3. All these hydrogels exhibit a crystalline structure with peaks angle around $2\theta = 9.8^\circ$, 19.6°, 26.6°. The pattern of hemicelluloses/PVA/chitin nanowhiskers shows two sharp diffraction peaks at about $2\theta = 19.6^\circ$, 26.6°, which are typical fingerprints of PVA, and the chitin nanowhiskers have a major crystalline peak at $2\theta = 9.8^\circ$.

The intensity of this reflection increased slightly with the increasing times of freeze/thaw cycle, indicating that the amount of crystalline phase was also increased. An increase of the number of freeze/thaw cycles improved the stability of the three polymers chains embedded mutually in the network. In the freshly prepared gels, the relative amount of "free water" decreased with increasing the number of freeze/thaw cycles, whereas in the rehydrated

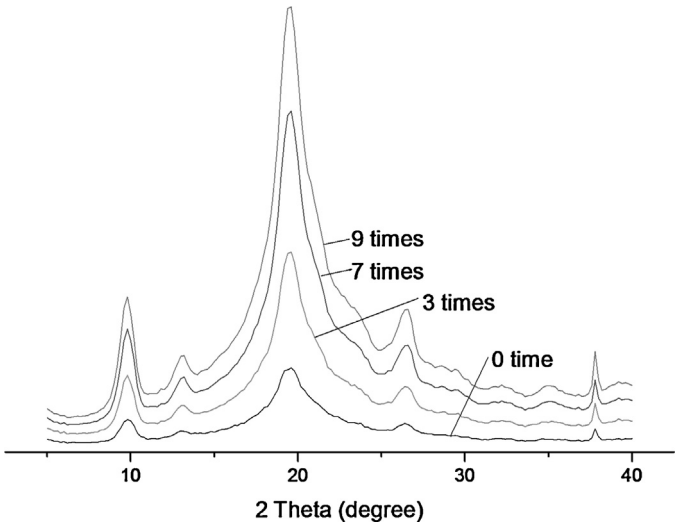

Fig. 3. X-ray diffraction patterns of Gel-0, Gel-3, and Gel-9.

samples is nearly constant (Ricciardi, Auriemma, & Rosa, 2005a). These structures of freeze/thaw hydrogels in terms of a porous polymer network where the crystals act as knots, the polymer segments ensure the connectivity all over the macroscopic hydrogel sample, while free water fills the pores. Water also acts as a swelling agent in the disordered zones of polymer matrix forming hydrogen bonds with the hydroxyl groups of the three polymers. The crystalline knots ensure high thermal stability and mechanical properties of the hydrogel (Jeanene Willcox et al., 1999; Yokoyama, Masada, Shimamura, Ikawa, & Monobe, 1986). This process of the hydrogel formation can be illustrated in Fig. 4.

Fig. 5A shows the FT-IR spectra of the chitin nanowhiskers, hemicelluloses, PVA, and Gel-3. The peaks at 1655 and 1621 cm^{-1} are assigned to the amide I region of α-chitin, and the peak at 1551 cm^{-1} is attributed to the amide II region of α-chitin (Goodrich & Winter, 2007). The characteristic bands of PVA at 1087, 1435 cm^{-1} are assigned to stretching vibration of C—O—C and to the $—CH_2$ bending, respectively. In the spectrum of hemicelluloses (Fig. 5A-b), the peak at about 3400 cm^{-1} is indicative of the stretching of the hydroxyl groups (Yang, Liu, Wang, & Song, 2010). The band at 1592 cm^{-1} is originated from $—COO^-$ of uronic acid and uronic carboxylate in hemicelluloses (Marchessault & Liang, 1962). The band at 1048 cm^{-1} is attributed to the C—O bond stretching frequencies. A band at 895 cm^{-1} is due to β-glycosidic linkages between the sugar units (Ebringerová, Hromádková, Alföldi, & Berth, 1992).

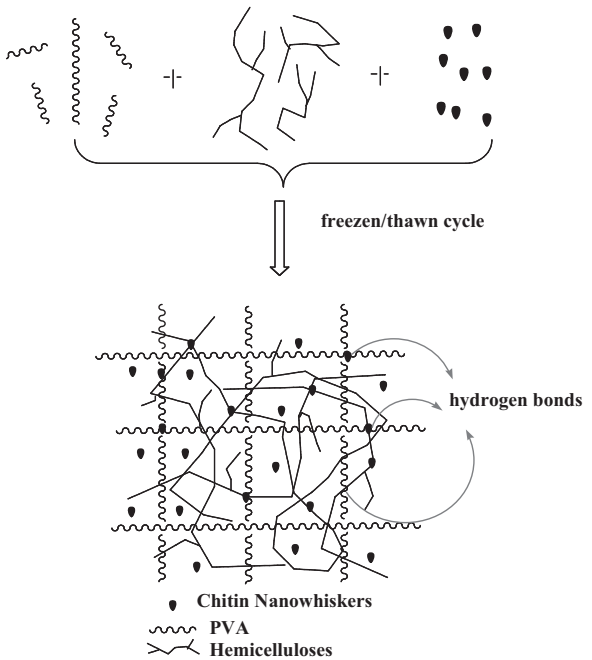

Fig. 4. Gelation mechanism of hemicelluloses, PVA, and chitin nanowhiskers in 6 freeze/thaw process.

In the FT-IR spectra of the blended hydrogel (Fig. 5A-d), two peaks at 1655 and 1621 cm^{-1}, which are assigned to the amide I region of chitin, were absent in the blend hydrogel. The typical signal of PVA at 1435 cm^{-1} was shifted to 1421 cm^{-1}, and the peak intensity at 1087 cm^{-1} decreased from spectrum c to spectrum d. In addition, the intensive peak at 1606 cm^{-1} is assigned to the H—O—H angle vibration originated from hydrogen bonds among the three polymers by freeze/thaw method (Haxaire, Maréchal, Milas, & Rinaudo, 2003), which is the overlap of the absorption at 1592 cm^{-1} by $—COO^-$ of uronic acid and uronic carboxylate. All these phenomenons could be implied that the hydrogel networks were formed by the three polymers. The hydroxyl group stretching vibration exhibited a strong absorption peak centered at about 3350 cm^{-1}, which indicated that significant hydrogen bonds were formed by freeze/thaw cycles. A physical reaction possibly occurred among hemicelluloses, PVA, and chitin nanowhiskers, and hydrogen bonds were formed by the freeze/thaw cycles. As there are no new peaks observed, it can be deduced that there is no chemical interaction among them. It can then be inferred that hemicelluloses, PVA, and chitin nanowhiskers have a physical interaction with the forming of hydrogen bonding. The chains of hemicelluloses, PVA, and chitin nanowhiskers were just physically entangled to form the networks.

The FT-IR of three hydrogels with 0, 3, and 9 times of repeated freeze/thaw cycle are displayed in Fig. 5B. From these curves, the absorption peak at the range of 3318–3337 cm^{-1}, which is assigned to hydroxyl group, becomes broader with the increment of the time of freeze/thaw cycles. This phenomenon indicated that hydrogen bond was formed tightly by physical reaction after each freeze/thaw cycle. In addition, there were no more changes among the three curves. It was confirmed that there was no chemical reaction occurred with the increasing of the freeze/thaw cycles.

3.3. Thermal properties

TGA is a powerful technique to determine the state of polymers and evaluate the inter-molecular interaction among polymers in the hydrogel. TGA and derivative thermo-gravimetric (DTG) thermogram of the two hydrogels with 0 and 3 times of freeze/thaw cycle are shown in Fig. 6. The curves of the two samples with several weight-loss steps were due to different influences to the degradation of hydrogel, such as water evaporation and hydrogel degradation. The weight loss below 100 °C was mostly attributed to the release of moisture from the samples.

As can be seen from the TGA curves, when temperature reached to 700 °C, the remaining solid residues were 12.9% for Gel-0, and 11.2% for Gel-3. The difference of maximum decomposition rates between Gel-0 and Gel-3 was shown in the DTG curves: two peaks with T_{max} (the decomposition temperature corresponding to the maximum weight loss rate) were present at 300 and 370 °C for Gel-0, 315 and 375 °C for Gel-3, respectively. In literatures, the T_{max} of hemicelluloses was 285 °C (Peng, Ren, Zhong, & Sun, 2011), the degradation temperature of PVA was 230 °C (Nata, Wang, Wu, & Lee, 2012), and two degradation peaks of chitin nanowhiskers were present at 200 and 360 °C (Samal, Chiellini, Bartoli, Fernandes, & Chiellini, 2009). Evidently, compared with these results, the degradation temperature increased significantly,

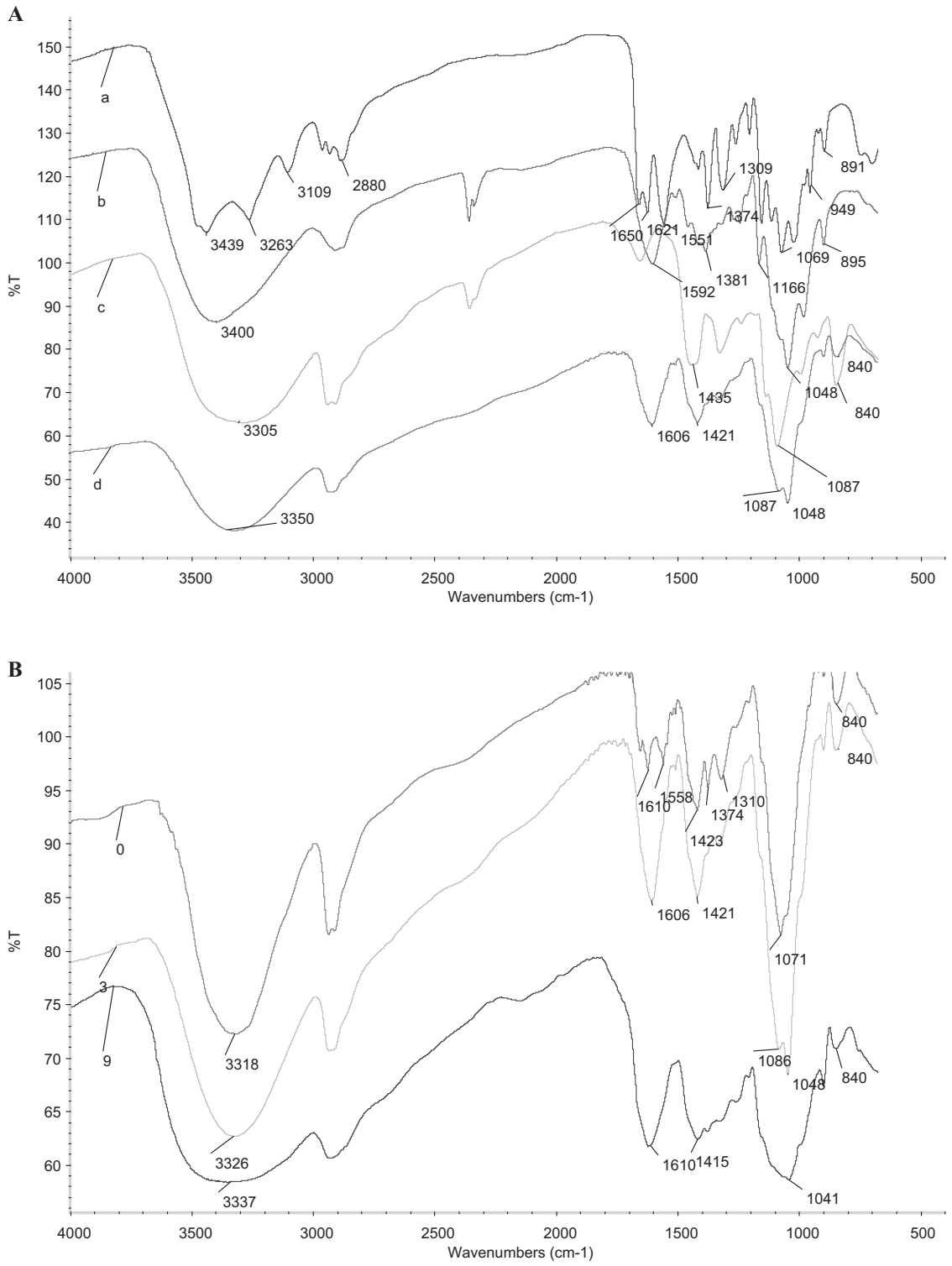

Fig. 5. (A) FT-IR spectra of NCH (a), hemicelluloses (b), PVA (c), and Gel-3 (d) and (B).FT-IR spectra of Gel-0, Gel-3, and Gel-9.

which was due to the formation of hydrogels with hemicelluloses, PVA, and chitin nanowhiskers. In other words, the freeze/thaw cycle hydrogels had a higher thermal stability than any of the three polymers. These results indicated that the thermal stability of the hydrogels was improved by the formation of hydrogen bonds among the polymers. The areas of the two peaks in Gel-3 were higher than that in Gel-0. The fact that the Gel-3 had higher thermal stability was mainly because of the presence of crystal structures, which was in accordance with the results of XRD.

3.4. The mechanical and swelling of hydrogels

The mechanical properties of hydrogels are important factors, which affect their actual applications. The stress–strain curves of the hydrogels with different freeze/thaw cycles are illustrated in

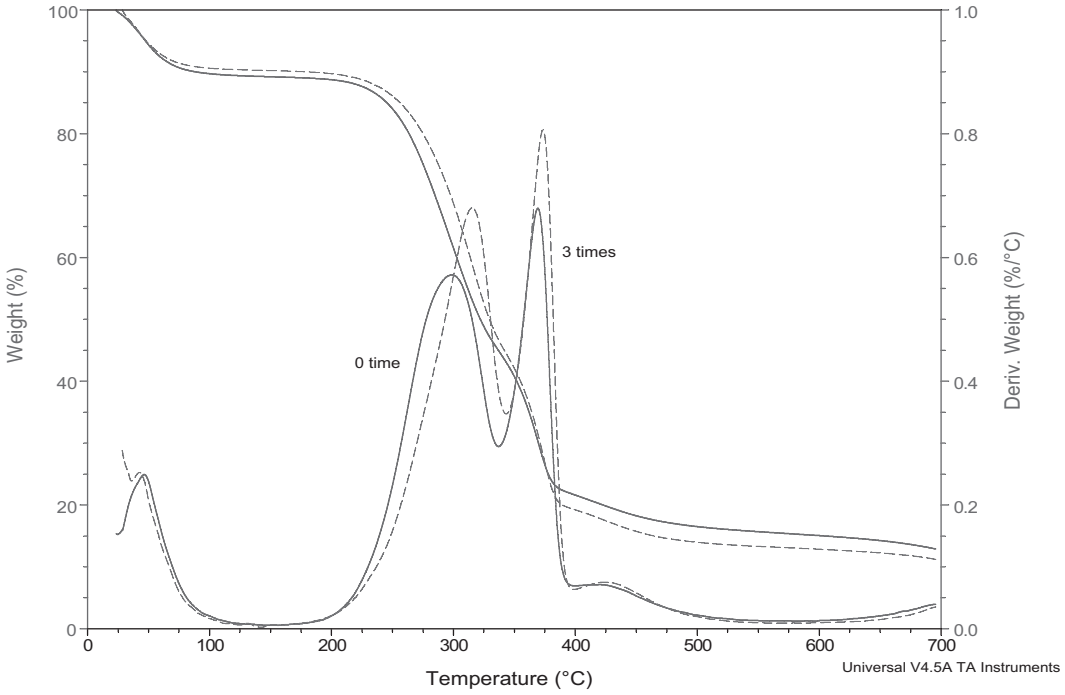

Fig. 6. TGA and DTG thermogram of Gel-0 and Gel-3.

Fig. 7. All hydrogels exhibited "J" shape curves with high compressive strength. The compressive strength of the freeze/thaw cycles increased with an increase of the applied load, but the compressive strength of Gel-3 was almost the same as that of Gel-7. The Gel-9 presented the highest compressive stress at 10.5 MPa, which was due to the stiff chains in the strong pore wall. Crosslink density of the blend hydrogels increased with the increasing of freeze/thaw cycles. It could be concluded that the hydrogels with higher crosslink density possess higher compressive strength, and more excellent compression resistance capability. This was because a highly crosslinked structure could not only increase stiffness of the hydrogels but also prevent water release from the hydrogels during the compressive testing, while the water in the hydrogel behaves as an incompressible fluid to resist compression.

The compressive stress of the prepared hydrogels in the present study was notably higher than that of the PVA hydrogel reported previously. Ricciardi et al. (2005b) prepared PVA hydrogel and found that the compressive stress of the PVA hydrogel with 9 times freeze/thaw cycle was nearly 2 MPa. It can be concluded that the hydrogels prepared by hemicelluloses, PVA, and chitin nanowhiskers exhibited good mechanical strength, which makes them good candidates for tissue engineering biomaterials.

As is well-known, compressive strength is consistent with the equilibrium swelling ratio. The equilibrium swelling ratios of the hydrogels are illustrated in Fig. 8. When the freeze/thaw cycles increased from 1 to 3 times, the equilibrium swelling ratio increased from 13.6 to 21.1 ($g\,g^{-1}$), whereas with the increment of the freeze/thaw cycles from 3 to 9 times, the equilibrium swelling ratio of the hydrogel samples decreased from 21.1 to 14.0 ($g\,g^{-1}$). The equilibrium swelling ratio of hydrogels decreased when the times of freeze/thaw cycles was above 3, which indicated that multiple freeze–thaw cycles resulted in a more compact network structure and less space in the polymeric matrix to accommodate water. Therefore, the swelling ratios are negatively related to the times of freeze–thaw cycle. A critical analysis of the swelling of hydrogel reveals three continuous processes: (1) penetration of the solvent molecules to the inside of hydrogel network, (2) relaxation of polymer chains, and (3) stretch of whole hydrogel network in solution (Tanaka & Fillmore, 1979).

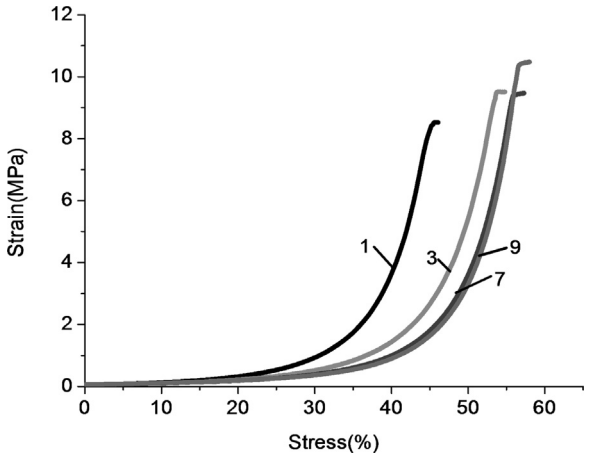

Fig. 7. The stress–strain curves of Gel-1, Gel-3, Gel-7, and Gel-9.

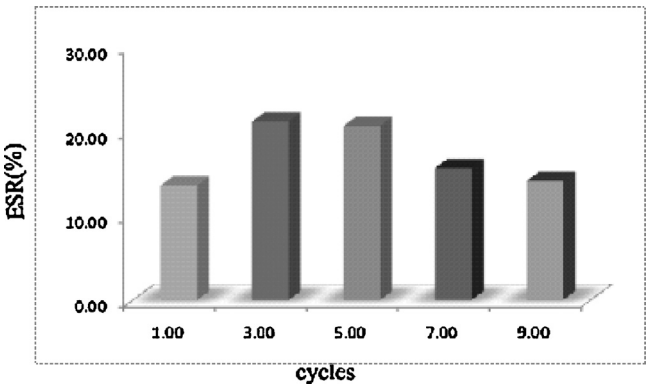

Fig. 8. The equilibrium swelling ratio of Gel-1, Gel-3, Gel-5, Gel-7, and Gel-9.

4. Conclusions

Chitin nanowhiskers with average length of 200 nm and average width of 40 nm were prepared through acid hydrolysis. Hydrogels were prepared by blending the hemicelluloses, polyvinyl alcohol (PVA), and chitin nanowhiskers through freeze/thaw technique without any chemical modification. Repeated freezing/thawing cycles induced the physically crosslinked chains packing of the three polymers (hemicelluloses, PVA, and chitin nanowhiskers) through the formation of intermolecular hydrogen-bonds. The chitin nanowhiskers were embedded homogeneously in the PVA/hemicelluloses matrix and restricted the packing and syneresis process, leading to the improvement of the thermal stability, compressive strength, and crystallinity of the hydrogels. In general, the increase of freezing/thawing cycles resulted in the more stiff structure, more stable thermal property, and higher crystalline degree, whereas after 3 times of freeze/thaw cycle, the equilibrium swelling ratio of hydrogels decreased due to the formation of the lamellar structure. The hydrogels with non-toxicity and biocompatibility have potential applications in tissue engineering and other biomaterials fields.

Acknowledgments

This work was supported by the grants from the Fundamental Research Funds for the Central Universities (No. 446 TD2011-11), Postdoctoral Science Foundation of China (2012M510328), Science Foundation for the Excellent Youth Scholars of Ministry of Education of China (20110014120006), Ministry of Science and Technology (973 project, 2010CB732203), the Natural Science Foundation of China (No. 30930073).

References

Andrade-Vivero, P., Fernandez-Gabriel, E., Alvarez-Lorenzo, C., & Concheiro, A. (2007). Improving the loading and release of NSAIDs from pHEMA hydrogels by copolymerization with functionalized monomers. *Journal of Pharmaceutical Sciences*, *96*, 802–813.

Bos, G. W., Jacobs, J. J. L., Koten, J. W., Van Tomme, S., Veldhuis, T., van Nostrum, C. F., et al. (2004). In *situ* crosslinked biodegradable hydrogels loaded with IL-2 are effective tools for local IL-2 therapy. *European Journal of Pharmaceutical Sciences*, *21*, 561–567.

Bouhadir, K. H., Kruger, G. M., Lee, K. Y., & Mooney, D. J. (2000). Sustained and controlled release of daunomycin from cross-linked poly(aldehyde guluronate) hydrogels. *Journal of Pharmaceutical Sciences*, *89*, 910–919.

Cai, S., Liu, Y., Zheng, S. X., & Prestwich, G. D. (2005). Injectable glycosaminoglycan hydrogels for controlled release of human basic fibroblast growth factor. *Biomaterials*, *26*, 6054–6067.

Camci-Unal, G., Alemdar, N., Annabi, N., & Khademhosseini, A. (2013). Oxygen-releasing biomaterials for tissue engineering. *Polymer International*, *62*, 843–848.

Chen, J., Park, H., & Park, K. (1999). Synthesis of superporous hydrogels: Hydrogels with fast swelling and superabsorbent properties. *Journal of Biomedical Materials Research*, *44*, 53–62.

Clark, G. L., & Smith, A. F. (1936). X-ray diffraction studies of chitin, chitosan, and derivatives. *The Journal of Physical Chemistry*, *40*, 863–879.

Coviello, T., Matricardi, P., Marianecci, C., & Alhaique, F. J. J. (2007). Polysaccharide hydrogels for modified release formulations. *Journal of Controlled Release*, *119*, 5–24.

Ebringerová, A., Hromádková, Z., Alföldi, J., & Berth, G. (1992). Structural and solution properties of corn cob eteroxylans. *Carbohydrate Polymer*, *19*, 99–105.

Galeska, I., Kim, T. K., Patil, S., Bhardwaj, U., Chatttopadhyay, D., Papadimitrakopoulos, F., et al. (2005). Controlled release of dexamethasone from PLGA microspheres embedded within polyacid-containing PVA hydrogels. *The AAPS Journal*, *7*, E231–E240.

Goodrich, J. D., & Winter, W. T. (2007). α-Chitin nanocrystals prepared from shrimp shells and their specific surface area measurement. *Biomarcromolecules*, *8*, 252–257.

Habibi, Y., Lucia, L. A., & Rojas, O. (2010). Cellulose nanocrystals: Chemistry, self-assembly, and applications. *Journal of Chemical Reviews*, *110*, 3479–3500.

Hassan, C. M., & Peppas, N. A. (2000). Structure and applications of poly(vinyl alcohol) hydrogels produced by conventional crosslinking or by freezing/thawing methods. *Advances in Polymer Science*, *153*, 37–65.

Haxaire, K., Maréchal, Y., Milas, M., & Rinaudo, M. (2003). Hydration of polysaccharide hyaluronan observed by IR spectrometry I. Preliminary experiments and band assignments. *Biopolymers*, *72*, 10–20.

Hoare, T. R., & Kohane, D. S. (2008). Hydrogels in drug delivery: Progress and challenges. *Polymer*, *49*, 1993–2007.

Jeanene Willcox, P., Howie, D. W., Jr., Schimdt-Rohr, K., Hoagland, D. A., Gido, S. P., Pudjijanto, S., et al. (1999). Microstructure of poly(vinyl alcohol) hydrogels produced by freeze/thaw cycling. *Journal of Polymer Science Part B*, *37*, 3438–3454.

Junkasem, J., Rujiravanit, R., Grady, B. P., & Supaphol, P. (2010). X-ray diffraction and dynamic mechanical analyses of α-chitin whisker-reinforced poly(vinyl alcohol) nanocomposite nanofibers. *Polymer International*, *59*, 85–91.

Junkasem, J., Rujiravanit, R., & Supaphol, P. (2006). Fabrication of α-chitin whisker-reinforced poly(vinyl alcohol) nanocomposite nanofibres by electrospinning. *Nanotechnology*, *17*, 4519–4528.

Lindblad, M. S., Sjoberg, J., Albertsson, A. C., & Hartman, J. (2007). Materials, chemicals and energy from forest biomass. In D. S. Argyropoulos (Ed.), *ACS symposium series 954* (pp. 153–167). Washington, DC: American Chemical Society.

Liu, J., Lin, S., Li, L., & Liu, E. (2005). Release of theophylline from polymer blend hydrogels. *International Journal of Pharmaceutics*, *298*, 117–125.

Liu, Y., Vrana, N. E., Cahill, P. A., & McGuinness, G. B. (2009). Physically crosslinked composite hydrogels of PVA with natural macromolecules: Structure, mechanical properties, and endothelial cell compatibility,. *Journal of Biomedical Materials Research Part B*, *90*, 492–502.

Lozinsky, V. I. (1998). Cryotropic gelation of poly(vinyl alcohol) solutions. *Russian Chemical Reviews*, *67*, 573–586.

Marchessault, R. H., & Liang, C. Y. (1962). The infrared spectra of crystalline polysaccharides. VIII. Xylans. *Journal of Polymer Science*, *59*, 357–378.

Michael, J. M. G., Clement, L. H., Luke, M. G., & Michael, J. D. N. (2009). The synthesis of novel pH-sensitive poly(vinyl alcohol) composite hydrogels using a freeze/thaw process for biomedical applications. *International Journal of Pharmaceutics*, *372*, 154–161.

Muzaffer, A. K., Mandla, A. T., Daniel, J. Y., & Gisela, B. D. (2011). Nanoreinforced biocompatible hydrogels from wood hemicelluloses and cellulose whiskers. *Carbohydrate Polymers*, *86*, 192–201.

Nata, I. F., Wang, S. S., Wu, T. M., & Lee, C. K. (2012). Carbonaceous hydrogels based on hydrothermal carbonization of glucose with chitin nanofibers. *Soft Matter*, *8*, 3522–3525.

Nishi, K. K., & Jayakrishnan, A. (2007). Self-gelling primaquine-gum arabic conjugate: An injectable controlled selivery aystem for primaquine. *Biomacromolecules*, *8*, 84–90.

Oxley, H. R., Corkhill, P. H., Fitton, J. H., & Tighe, B. J. (1993). Macroporous hydrogels for biomedical applications: Methodology and morphology. *Biomaterials*, *14*, 1064–1072.

Peng, F., Ren, J. L., Xu, F., Bian, J., Peng, P., & Sun, R. C. (2009). Comparative study of hemicelluloses obtained by graded ethanol precipitation from sugarcane bagasse. *Journal of Agriculture and Food Chemistry*, *57*, 6305–6317.

Peng, X. W., Ren, J. L., Zhong, L. X., & Sun, R. C. (2011). Nanocomposite films based on xylan-rich hemicelluloses and cellulose nanofibers with enhanced mechanical properties. *Biomacromolecules*, *12*, 3321–3329.

Peppas, N. A. (1975). Turbidimetric studies of aqueous poly(vinyl alcohol) solutions. *Macromolecular Chemistry and Physics*, *176*, 3433–3439.

Peppas, N. A. (1979). Characterization of homogeneous and pseudocomposite homo polymers and co polymers for articular cartilage replacement. *Biomaterials Medical Devices and Artificial Organs*, *7*, 421–442.

Ricciardi, R., Auriemma, F., & Rosa, C. D. (2005). Structure and properties of poly(vinyl alcohol) hydrogels obtained by freeze/thaw techniques. *Macromolecular Symposia*, *222*, 49–64.

Ricciardi, R., Errico, D., Auriemma, G., Ducouret, F., Tedeschi, G., Rosa, A. M., et al. (2005). Short time dynamics of solvent molecules and supramolecular organization of poly(vinyl alcohol) hydrogels obtained by freeze/thaw techniques. *Macromolecules*, *38*, 6629–6639.

Saito, Y., Putaux, J. L., Okano, T., Gaill, F., & Chanzy, H. (1997). Structural aspects of the swelling of β-chitin in HCl and its conversion into α-chitin. *Macromolecules*, *30*, 3867–3873.

Samal, S. K., Chiellini, F., Bartoli, C., Fernandes, E. G., & Chiellini, E. (2009). Hybrid hydrogels based on poly(vinyl alcohol)-Chitosan blends and relevant CNT composites. In *Hydrogels: Biological Properties and Applications* (pp. 67–78). Milan: Springer.

Slaughter, B. V., Khurshid, S. S., Fisher, O. Z., Khademhosseini, A., & Peppas, N. A. (2009). Hydrogels in regenerative medicine. *Advanced Materials*, *21*, 3307–3329.

Tamuraa, H., Furuikea, T., Nairb, S. V., & Jayakumar, R. (2011). Biomedical applications of chitin hydrogel membranes and scaffolds. *Carbohydrate Polymers*, *84*, 820–824.

Tanaka, T., & Fillmore, D. J. (1979). Kinetics of swelling of gels. *Journal of Chemical Physics*, *70*, 1214–1218.

Tang, H., Zhou, W. J., & Zhang, L. N. (2012). Adsorption isotherms and kinetics studies of malachite green on chitin hydrogels. *Journal of Hazardous Materials*, *209–210*, 218–225.

Ushio, K., Oka, M., Hyon, S., Hayami, T., Yura, S., Matsumura, K., et al. (2004). Attachment of artificial cartilage to underlying bone. *Journal of Biomedical Materials Research Part B: Applied Biomaterials*, *68B*, 59–68.

Wichterle, O., & Lím, D. (1960). Hydrophilic gels for biological use. *Nature*, *185*, 117–118.

Yang, S. W., Liu, G. Q., Wang, X. Q., & Song, J. Y. (2010). Electroresponsive behavior of a sulfonated poly(vinyl alcohol) hydrogel and its application

to electrodriven artificial fish. *Journal of Applied Polymer Science*, *117*, 2346–2353.

Yeo, J. H., Lee, K. G., Kim, H. C., OH, Y. L., Kim, A. J., & Kim, S. Y. (2000). The effects of PVA/chitosan/fibroin(PCF)-blended spongy sheets on wound healing in rats. *Biological and Pharmaceutical Bulletin*, *23*, 1220–1223.

Yokoyama, F., Masada, I., Shimamura, K., Ikawa, T., & Monobe, K. (1986). Morphology and structure of highly elastic poly(vinyl alcohol) hydrogel prepared by repeated freezing-and-melting. *Colloid and Polymer Science*, *264*, 595–601.

Zeng, J. B., He, Y. S., Li, S. L., & Wang, Y. Z. (2012). Chitin whiskers: An overview. *Biomacromolecules*, *13*, 1–11.